PERFORMANCE OF NATURAL ZEOLITE AND SEPIOLITE IN THE REMOVAL OF FREE CYANIDE AND COPPER-COMPLEXED CYANIDE ($[Cu(CN)_3]^{2-}$)

ESRA TARLAN-YEL[1],* AND VILDAN ÖNEN[2]

[1] Department of Environmental Engineering, Selcuk University, 42075 Campus-Konya, Turkey
[2] Department of Mining Engineering, Selcuk University, 42075 Campus-Konya, Turkey

Abstract—The chemical and biological methods employed to date in the removal of free cyanide (CN^-) and metal-cyanide complexes from aqueous fluids have proved expensive and problematic. A simpler and more economical approach was attempted in the present study using zeolite and sepiolite. The effectiveness of zeolite from Manisa-Gördes (Turkey) and of sepiolite Eskişehir-Sivrihisar (Turkey) at removing free and Cu-complexed cyanide, $[Cu(CN)_3]^{2-}$ was investigated. For removal of CN^-, the system performance was examined in terms of concentration, particle size, and retention time. Material with smaller particle sizes (<0.106 mm) performed better, particularly in the case of sepiolite. The maximum CN^- removal capacities of zeolite and sepiolite were calculated as 571 and 695 meq/100 g for free CN adsorption, and 455 and 435 meq/100 g for Cu-complexed CN adsorption, respectively. The time to reach equilibrium was calculated as 1050 min. Acid activation, a simple cation adsorption removal method, did not improve the process, instead leading to reduced CN adsorption. Hydroxylated surfaces of metal oxides at the edges of zeolite develop charges and exchange with anions in water. Mg^{2+} ions located at the edges of the octahedral sheet can create complexes with CN^- anions. Moreover, hydrogen bonding with anions (CN^- in this case) and H^+ of zeolitic water bonded to coordinated water molecules can also create complexes. These two complexes are considered to be effective mechanisms for sepiolite. The effects of both acid activation and CN adsorption were clearly observed in the Fourier-transform infrared spectra. Removal of CN was characterized by the Langmuir isotherm, indicating monolayer coverage with chemical bonding to the surface, which deteriorated during acid activation. The study indicated that zeolite and sepiolite can be used efficiently and easily for removal of free and Cu-complexed CN.

Key Words—Acid Activation, Cu-complexed, Cyanide, Free Cyanide, Removal, Sepiolite, Zeolite.

INTRODUCTION

Cyanide species are notable pollutants because of their toxicity and their ability to form a number of chemical compounds and complexes. Three groups of cyanide species exist in wastes, namely: free cyanides (CN^-), metal-cyanide complexes (*Me*-CN), and other compounds formed from cyanide reactions. *Me*-CN release CN^- ions under low-pH conditions which increases the toxic effects of the solution. Copper is a major cyanide complexing metal and each of the complexes formed has high solubility. Some notable Cu complexes are $Cu(CN)_2^-$, $Cu(CN)_3^{2-}$, and $Cu(CN)_4^{3-}$ (Barakat, 2005).

Degradation is used in the removal of cyanide from wastewaters (Young and Jordan, 1995). Three main degradation mechanisms have been applied: natural, chemical, and biological processes. Natural degradation is widely applied in tailing dams, employing separation of complexes through photodegradation, oxidation, and sedimentation mechanisms (Ou and Zaidi, 1995) releas-ing free forms into the atmosphere. The most common chemical degradation process, which is very expensive, is oxidation (Robbins and Devuyst, 1995; Yarar, 2001). Oxidation has operational difficulties and other disadvantages such as chemical requirements. Biological degradation is achieved through metabolic and enzymatic oxidation and metabolic adsorption (Yarar, 2001; Young and Jordan, 1995) to by-products such as ammonia, thiocyanate, and metal ions (Waterland, 1995). The main drawbacks of biological CN^- treatment are, again, operational, with significant treatment costs because of the use of chemicals and the safety precautions required (Waterland, 1995; Yarar, 2001).

A more feasible method for the removal of cyanide compounds generated by industrial processes and mining activities is needed. In the literature, cation (especially metals) and cyanide removal using natural materials such as zeolite and clays has been studied (Baghel *et al.*, 2006; Barakat, 2005; Brigatti *et al.*, 1999, 2000), but their use is limited, especially for anions (Özdemir *et al.*, 2007; Sujana *et al.*, 2009) as they undergo both adsorption and ion exchange simultaneously. New applications of these natural materials are being developed, with possible application in wastewater-treatment processes.

Zeolites and sepiolites are abundant and cheap natural materials for use in environmental technologies,

especially in advanced treatment applications (including sorption) due to their chemical properties, crystal structures, and large interior surface areas (300−600 m²/g for zeolites and ~340 m²/g for sepiolites) (Brigatti *et al.*, 2000; Shariatmadari *et al.*, 1999; Rytwo *et al.*, 1998; Tijburg and Konuksever, 1998). Thus far, use of these natural materials for this purpose has been limited even though they can be used both as a raw mineral and in activated form. Activation processes affect some of the chemical and surface properties of the minerals, resulting in changes in the selectivity of the mineral which can provide a greater degree of removal of some ions.

MATERIALS AND METHODS

Zeolite and sepiolite

Zeolite from the Manisa-Gördes (Turkey) region was obtained from the Enli Madencilik Co., Ltd., and sepiolite from the Eskişehir-Sivrihisar (Turkey) region was obtained from the Doğuş Madencilik Inc. Co. The Manisa-Gördes clinoptilolite is the most common natural zeolite belonging to the heulandite family and has the following general formula: $KNa_2Ca_2(Si_{29}Al_7)O_{72}.24H_2O$ established from its X-ray diffraction (XRD) pattern. The ratio of Si to Al (generally 4.0−5.3) (Kowalczyk e*t al.*, 2006) was 4.14 in the samples studied here. The crystal structure of the mineral is represented by a 3-dimensional aluminosilicate framework, the structure of which leads to micropores and channels occupied by water molecules and exchangeable cations. The specific surface area of the raw zeolite is 50 m²/g in this case.

The sepiolite from Eskişehir-Sivrihisar has the formula $Mg_4Si_6O_{15}(OH)_2.6H_2O$ and structurally consists of an alternation of blocks and tunnels which grew in the fiber direction. Each structural block comprises two tetrahedral silica sheets enclosing a central discontinuous octahedral sheet where Mg^{2+} ions occupy structural positions. Such Mg-rich sepiolite contains minor quantities of Al^{3+} and Fe^{3+} (<0.1%) in the tetrahedral sheet. The specific surface area was 293 m²/g for the raw sepiolite in this study.

Activation

As well as use of raw forms, the zeolite and sepiolite were also subjected to acid activation. 10 wt.% suspensions were prepared with solutions of 0.5, 0.75, 1.0, and 1.25 N HNO_3 of 65%; mixed for 6 h at 70ºC; then rinsed with distilled water until their pH value reached ~5.5. Following a thorough rinsing process the samples were filtered and dried at 60ºC. The dealumination of zeolite during the acid treatment can be represented by the following reaction (Barrer and Makki, 1964):
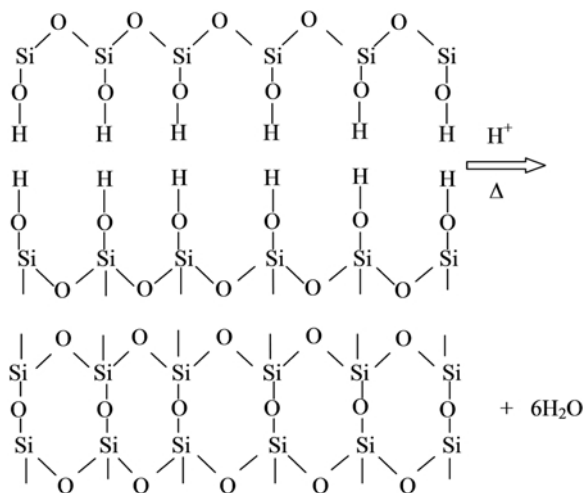
Similarly, the acid dissolution of sepiolite can be represented by the following reactions (Hernandez *et al.*, 1986):
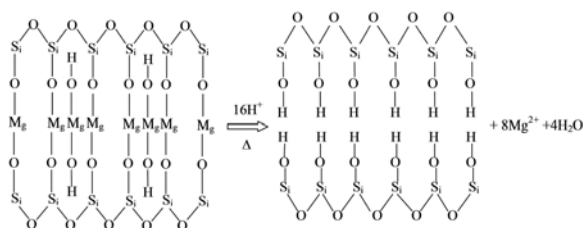
At the initial stage of acid treatment of zeolite, cations are discharged from exchange positions. In the next stage, the skeleton is dealuminated with no visible changes in the latter. At the final stage, disintegration of the skeleton is observed resulting in an amorphous phase (Vasylechko *et al*., 2003). Activation resulted in an increase in the specific surface area to 75 m²/g.

During acid activation, the specific surface area increases until the magnesium of the brucitic sheet has been extracted completely. As the dissolution of the magnesium layer of the reticulum of sepiolite occurs, textural changes are produced. Following the dissolution of the octahedral sheet, two new facing surfaces appear, which are highly reactive and contain a number of silanol groups susceptible to undergoing a condensation reaction with the formation of siloxane groups (Hernandez *et al.*, 1986). In >0.75 N acid solutions, the macro-pores in the sepiolite structure collapse and amorphous silica forms when all Mg in the structure dissolves into the solution. This collapse shortens the fibers (Çetişli and Gedikbey, 1990), and, therefore, in more acidic conditions, the specific surface area begins to decrease. In the present study, the specific surface area of sepiolite increased from 293 to 310 m²/g for 0.75 N and then decreased to 210 m²/g at 1.0 and 1.25 N.

The effects of acid activation on the surfaces of zeolite and sepiolite are clearly seen in the scanning

electron micrographs (SEM) of the raw and activated minerals (Figure 1).

Adsorption studies

Free CN, (CN^-), adsorption. Experiments were performed with stock CN^- solution prepared synthetically using KCN (obtained from Merck). The pH was adjusted with NaOH to 9 at the beginning of the experiments and controlled continuously. In batch studies, varying mineral dosages were applied to 200 mL solutions, including the same initial concentration of CN^-, and shaken at 220 rpm at a constant room temperature (20−22ºC). Samples taken at various time intervals were left to settle for 6 h and CN^- measurements were obtained from the supernatants. The effects of the initial concentration, particle size, and retention time were noted. Experiments were repeated with the acid-activated forms of both minerals.

For continuous studies, a slurry of 4 g of mineral was packed in a glass column of 1 cm inner diameter with a glass-wool support at the top and bottom. The bed height in the column was 8.5 cm. The CN^- solution concentration in the reservoir was 200 mg/L and the solution feed rate was adjusted to 20 mL/min using a pump. In order to obtain comparable results, the columns were operated under the same conditions in parallel tests for both zeolite and sepiolite. At various time intervals, samples were taken from the effluent and CN^- analysis performed.

Cu-complexed CN ($[Cu(CN)_3]^{2-}$) adsorption. The experiments were performed in a batch system containing 0.05 g of mineral in 100 mL of $[Cu(CN)_3]^{2-}$ solution. The desired solution concentrations were obtained by diluting aliquots from a 14.15 g/L (0.1 M concentration) stock solution prepared by dissolving commercially available CuCN in KCN solution under alkaline conditions. Flasks were then placed in the shaker at 220 rpm at room temperature (20−22ºC). In preliminary experiments, aqueous solutions were
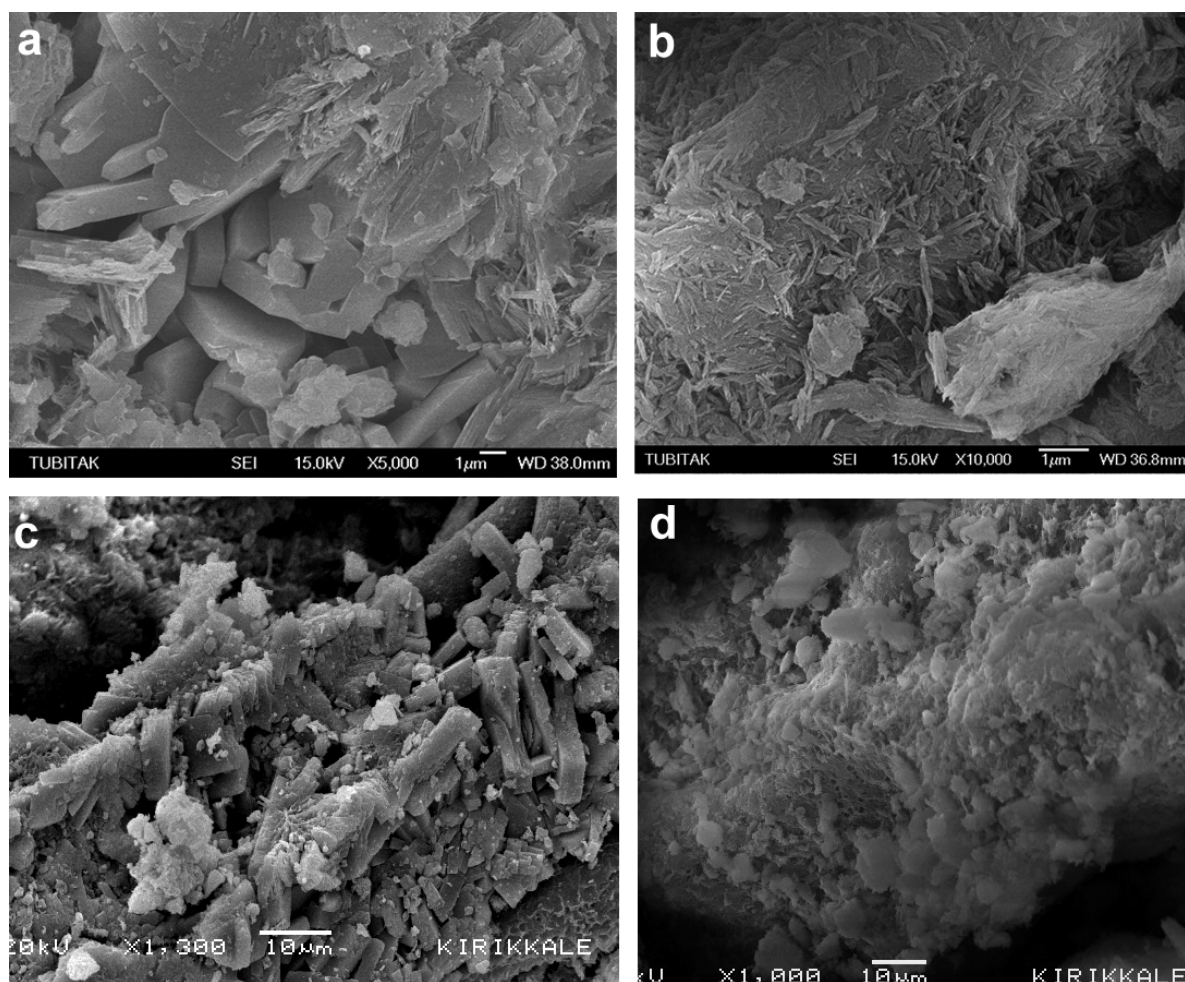

Figure 1. SEM images of (a) 0.106−0.300 mm raw zeolite, (b) 0.106−0.300 mm raw sepiolite, (c) 0.106−0.300 mm 0.5 N acid-activated zeolite, and (d) 0.106−0.300 mm 0.5 N acid-activated sepiolite.

sampled and the concentrations determined. At the time the samples showed no concentration difference, the system was considered to be at equilibrium.

Adsorption isotherm analyses

Adsorption isotherms are important in describing how adsorbates interact with the adsorbent and are useful for optimizing the use of zeolite and sepiolite as an adsorber. Analysis of equilibrium data for the adsorption of Cu-complexed CN on zeolite and sepiolite was conducted using the Langmuir, Tempkin, and Freundlich isotherms. Langmuir is the isotherm which assumes monolayer coverage in the specific adsorption sites on the surface. The Tempkin isotherm assumes that the adsorption enthalpy changes linearly with time, while Freundlich assumes a logarithmic change.

The experimental data were collected under different initial concentrations and isotherm plots were constructed according to linearized forms of each isotherm equation. Isotherm constants were then calculated and correlations compared.

Analyses

All analyses were performed according to Standard Methods (APHA, 1998). The CN^- analyses were performed by method 4500-CN. The pH values were measured using a pH meter (Jenway3060, 1 to 14 range). The FTIR spectra were obtained in the $4000-400$ cm^{-1} region using the KBr pellet technique (1% sample:KBr).

RESULTS AND DISCUSSION

Free CN, (CN$^-$), adsorption. In all trials under different mineral dosages and initial CN^- concentrations, both minerals, either raw or in the acid-activated form, were found to be effective at removing CN^-. Common to all experiments was the fact that the pH of the solutions, which was adjusted to 9 at the beginning, remained constant at ~9 after processing the mineral.

Smaller particles (<0.300 mm) were more effective at removing CN^- (Figure 2), for both batch and continuous adsorption reactors, with the exception of the packed bed arrangement. For sepiolite and zeolite, a particle size of <0.106 mm achieved better levels of CN^- removal than a larger particle size (0.106−0.300 mm); the effect was significantly greater in the case of sepiolite. The data also suggested that CN^- removal was rapid in the first 30 min and then decelerated. For zeolite, 64% CN was removed in the first 60 min. Removal continued, however, until equilibrium was reached at 1050 min at which time 83% of the CN had been removed. For sepiolite, 72% of the CN had been removed at the end of 60 min, but by the time equilibrium was reached at 1050 min, 99% had been removed. Retention time in a treatment unit is critical in terms of the overall (and targeted) efficiency of the wastewater treatment plant. The difference in degree of removal between 60 min and

1050 min for the <0.106 mm particle size for both minerals, at all initial conditions (Figure 3), means that the shorter times cannot be considered further in this experiment if more than 72% efficiency is required.

The three degradation methods mentioned in the introduction take from minutes to weeks to achieve completion, depending on the method, but also involve other chemicals or micro-organisms, increasing the cost and complexity.

The adsorption isotherm curves for CN^- adsorption (Figure 4) showed favorable adsorption for zeolite and sepiolite. As in Figure 3, the effect of particle size was clearly observed where smaller particle size resulted in greater CN^--removal capacities for both minerals. The maximum observed CN^--adsorption capacities were 530 and 695 meq/100 g at equilibrium for zeolite and sepiolite, respectively.

0.01w>In the case of acid activation, removal profiles were almost the same for both minerals (data not shown) though the capacities decreased to 504 meq/100 g for zeolite and to 533 meq/100 g for sepiolite. These capacity decreases were attributed to structural changes in the minerals during acid activation, explained in the 'Activation' section above, and in agreement with the findings of Vasylechko *et al.* (2003) and Hernandez *et al.* (1986). In general, acid activation is known to modify the surface structure of minerals to improve their adsorption and/or ion-exchange properties, though published studies have focused on cation-removal performance. Acid activation may have a positive influence on cation-exchange capacities, but not on anion-removal performance, indicating that anion removal is not directly related to the specific surface area of the mineral.

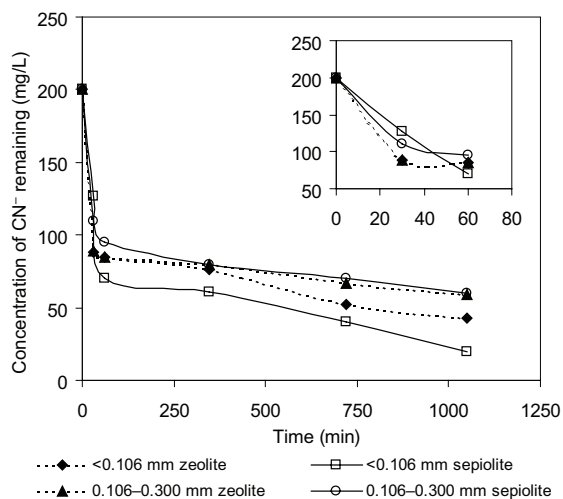Column studies, performed in a 1 cm inner-diameter column, provided breakthrough information (Figure 5).

Figure 2. Change in concentration of CN^- remaining with time and particle size for a dosage of 3 g/L zeolite and sepiolite.
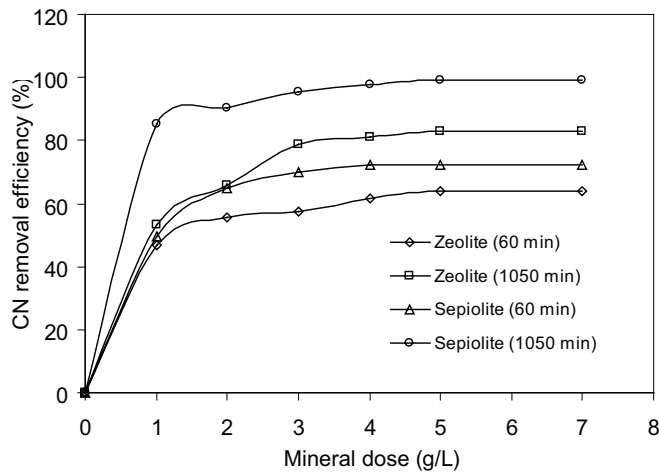

Figure 3. CN⁻-removal performance after 60 and 1050 min for <0.106 mm-sized minerals. 60 min marks the end of the initial, rapid removal, after which the removal rate decelerated.
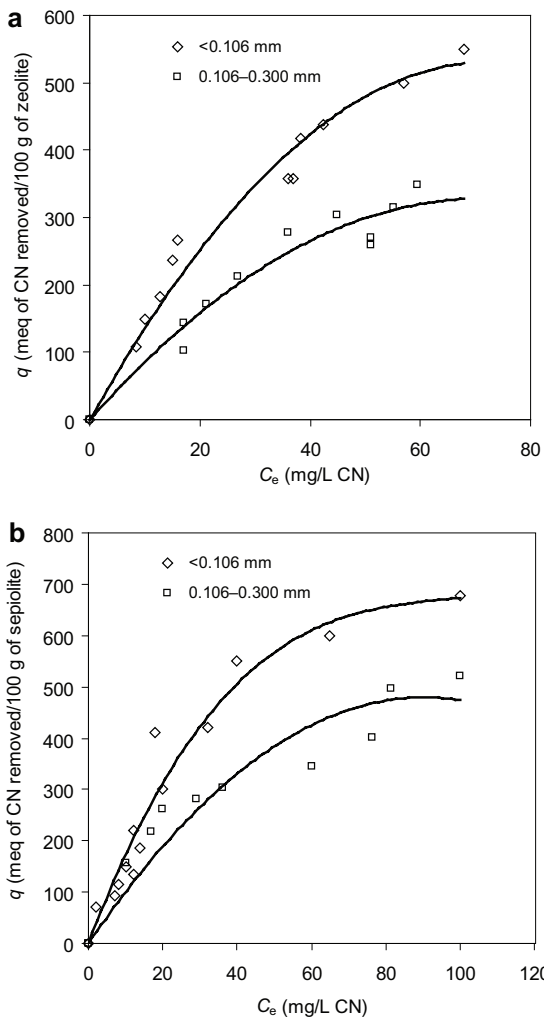

Figure 4. Adsorption isotherm curves for (a) zeolite, and (b) sepiolite at two different particle sizes. C_e = the effluent (CN) concentration.

The data were subjected to a kinetic approach, and column capacities were calculated with the help of a linearized form of the column design model 1 (Figure 6) (Reynolds, 1982).

$$C_o/C_e = 1 + \exp[k_1/Q(q_o{*}M - C_oV)] \qquad (1)$$

where C_o is the initial CN⁻ concentration = 200 mg/L (7.69 meq/L); C_e, the effluent CN⁻ concentration, mg/L (meq/L); k_1, the rate constant, L/d.meq; q_0, the CN⁻ uptake capacity, mg/g or meq/g; M, the mass of mineral = 4 g; Q, the flowrate = 0.02 L/min (28.8 L/d); and V, the throughput volume at time t, L. From the equation of the trendline of the linearized form of design equation 1 (Figure 6), the constants were established as $k_{1zeolite}$ = 6.61 L/d.meq, $k_{1sepiolite}$ = 6.32 L/d.meq, $q_{0zeolite}$ = 5.709 meq/g, and $q_{0sepiolite}$ = 6.82 meq/g, or, in other words, the calculated zeolite capacity was 571 meq/100 g while
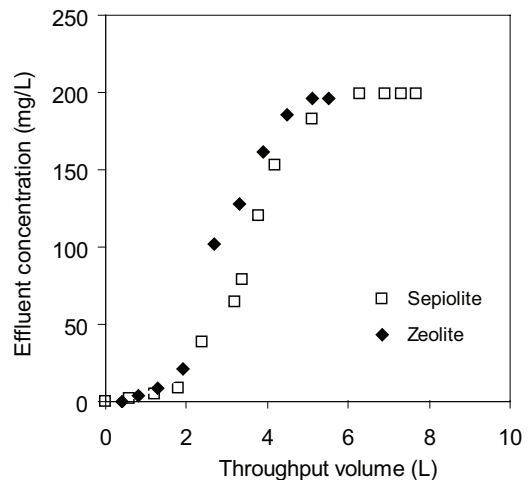

Figure 5. Breakthrough data for column studies.

that for sepiolite was 682 meq/100 g. The calculated capacities were consistent with those found in batch studies, and were sufficiently high for both zeolite and sepiolite considering the theoretically suggested (Reynolds, 1982) capacity interval (200−500 meq/100 g). In addition, 80−112 meq/100 g was reported as the maximum achievable CN^- adsorption capacity interval by Monser and Adhoum (2002), which was much smaller than that indicated by the present data.

Cu-complexed CN ($[Cu(CN)_3]^{2-}$) adsorption

In Cu-complexed CN removal, zeolite performed better in both the raw and activated mineral forms (Figure 7). Different activation conditions had no notable effect on the performance. Comparison of the effects of particle size on the resultant performances (Figure 7) found that zeolite was more effective than sepiolite at Cu-complexed CN removal under all activation conditions and particle sizes studied. These particle sizes were the best for adsorption reactors, either in batch or continuous columns, with the exception of the packed bed arrangement.

The presence of Cu in the medium affected CN^- ion behavior due to its complexing effect. Isotherm curves of zeolite and sepiolite for Cu-complexed CN adsorption (Figure 8) indicated favorable adsorption. The effect of activation is clearly seen in the CN^- data above, such that raw mineral forms resulted in a greater degree of Cu-complexed CN removal for both minerals. The observed maximum capacities were 455 and 435 meq/100 g at equilibrium for zeolite and sepiolite, respectively. Zeolite performed better at Cu-complexed CN removal with its consistent removal curves for both raw and activated mineral forms. Similar to the findings for free CN, activation decreased the removal performances to 345 and 303 meq/L, respectively, due to
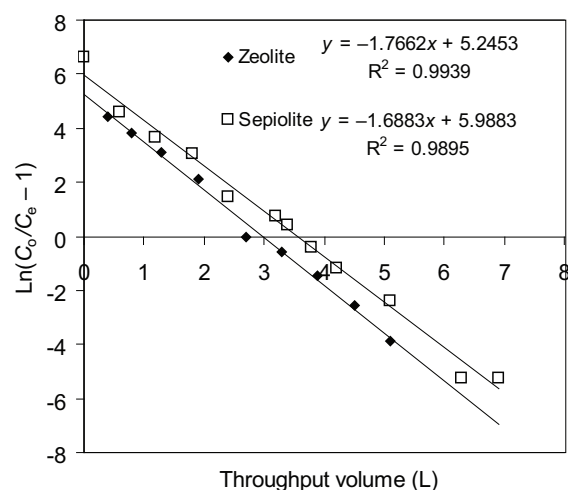
structural changes at the mineral surface during activation, as discussed above.

The coefficients of determination of linearized regression plots of the Freundlich, Langmuir, and Tempkin isotherms (Table 1) clearly indicated that the data fitted the Langmuir isotherm best, which contemplates chemisorption in a monolayer on the mineral surface with maximum capacities represented by q_m values. For all mineral conditions, the calculated monolayer adsorption capacities were similar to but slightly greater than experimental values (Table 1, Figure 8).

Overall performance comparison and mechanisms

The overall performance and capacity (summarized in Table 2) of the two minerals indicated that the formation of complexes altered their adsorptive behavior. Free CN was adsorbed more efficiently by sepiolite, whereas Cu-complexed CN was adsorbed better by zeolite. Acid activation adversely affected the adsorption performance of both. These minerals carry a negative surface charge, resulting in large cation exchange capacities (CEC), and are widely used in

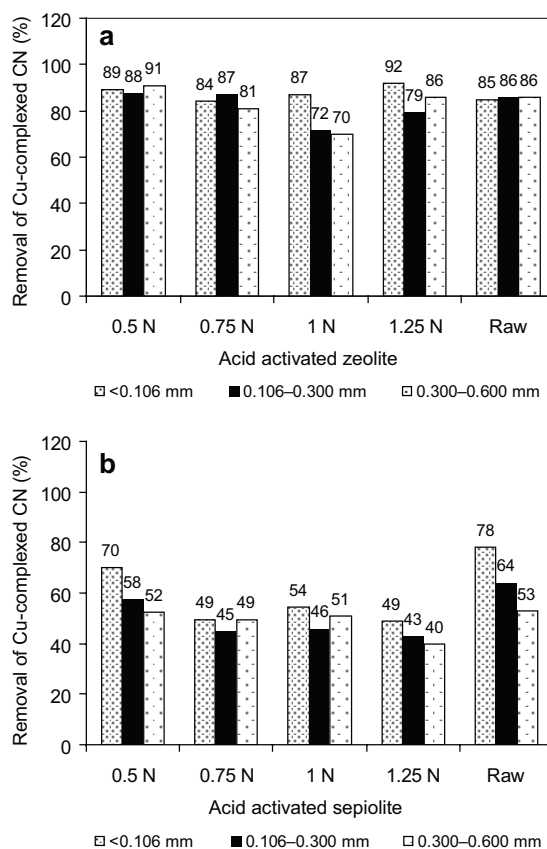Figure 6. Linearized form of column-design model (after Reynolds, 1982).

Figure 7. Effect of particle size on the removal efficiency of Cu-complexed CN of raw and acid-activated (a) zeolite and (b) sepiolite.
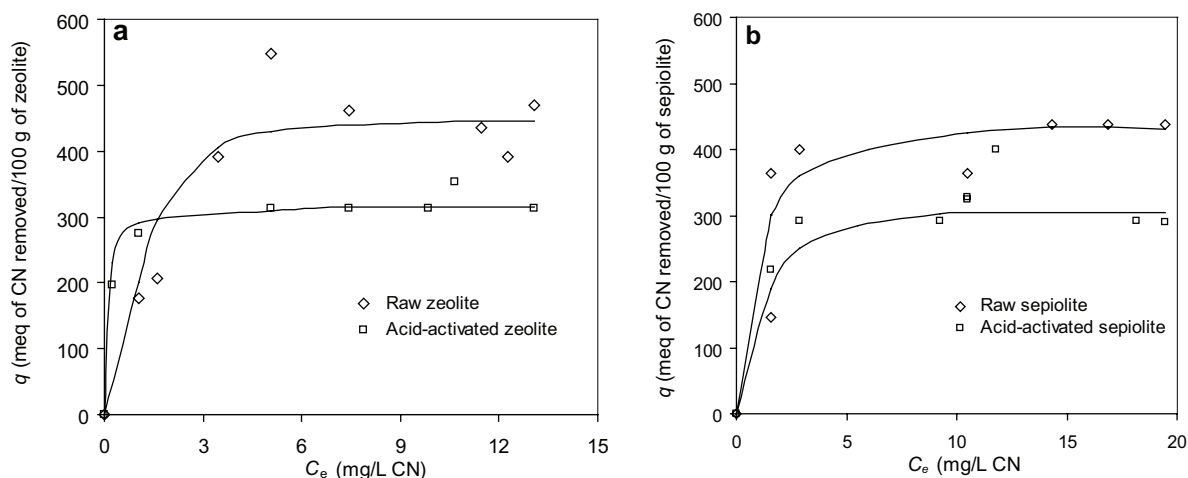
Figure 8. Adsorption isotherm curves for Cu-complexed CN adsorption of raw and acid-activated (a) zeolite and (b) sepiolite. C_e = the effluent (CN) concentration.

cation removal. On the other hand, CN compounds bear a negative charge, which prevents net attraction, resulting in great sorption. CN removal clearly was not related to simple cation adsorption. Technically, the two most important adsorption phenomena in clays are the cation exchange adsorption on the layer surfaces, and chemisorption of anions at the edge surfaces (van Olphen, 1959).

The zeolite layer edges are similar to the surfaces of hydrous oxides of Si and Al, which in an aqueous system are susceptible to complexation with ligands from solution. The charge at these layer edges is pH dependent. The specific sorption of anions by these oxide species may be modeled as a two-step ligand-exchange reaction, explained by Sujana *et al.* (2009), who reported an exchange of the surface hydroxide ion with the anion in the aqueous environment. At alkaline pH, due to competition between the OH ions and the anions for edge-surface sites, or due to electrostatic repulsion of anions from the negatively charged surface,

sorption is decreased. Both of these factors became more important after acid activation.

In the structure of sepiolite, Mg^{2+} ions were located at the edges of the octahedral sheet and zeolitic water bonded to coordinated water molecules through hydrogen bonding. Complexation between these Mg^{2+} ions and CN anions and/or hydrogen bonding anions and the H^+ of bound water occur; and passivation of the SiO_2/Si interface states by CN and defection of states in poly-Si by the formation of Si-CN bonds (Fujiwara *et al.*, 2004) are the main mechanisms for sepiolite. Dissolution of Mg together with the octahedral sheet and the decrease in zeolitic water after acid activation are the main reasons for the decreases in adsorption capacities.

These mechanisms are consistent with the findings of Özdemir *et al.* (2007) who suggested three adsorption modes for an anion: first is the complexation between the Mg ion at the edge of the octahedral sheet and polar anionic head groups or electrostatic attraction between the Mg ion and the polar head; second is the hydrogen

Table 1. Isotherm constants and correlations for the adsorption of Cu-complexed CN.

	Freundlich			Langmuir			Tempkin		
	k	$1/n$	r^2	b	q_m	r^2	A	RT/b	r^2
Raw sepiolite	117.5	0.20	0.29	0.022	500	**0.97**	156	48.15	0.26
Acid-activated sepiolite	89.1	0.23	0.43	0.3	333	**0.849**	0.15	71.37	0.37
Raw zeolite	117.5	0.25	0.50	0.029	500	**0.853**	0.32	84.40	0.35
Acid-activated zeolite	269.2	0.05	0.72	0.214	333	**0.992**	71438	33.34	0.88

r^2: coefficient of determination of each isotherm (bold indicates the fit of data to that isotherm)
k: adsorption capacity at unit concentration (meq/g)
$1/n$: adsorption intensity, dimensionless
b: relative energy of adsorption, L/meq
q_m: ultimate adsorption capacity of the mineral, meq/100 g
A: Tempkin isotherm constant
RT/b: heat of adsorption

Table 2. Comparison of CN and Cu-complexed CN adsorption for both minerals.

Mineral		Maximum CN^- adsorption capacity (meq/100 g)	Maximum Cu-complexed CN adsorption capacity (meq/100 g)
Zeolite	Raw	571	455
	Acid-activated	504	345
Sepiolite	Raw	695	435
	Acid-activated	533	303

bonding between the anionic polar head and H^+ of bound water or zeolitic water; and third is the chain–chain interaction leading to hemimicelle formation.

The degree of adsorption at the surface depends on the relative affinity of the ion for the mineral surface. For Cu-complexed CN, competitive adsorption occurs between two ions, strongly dependent on pH, and since pH was sufficiently high (9–9.5) for the soluble form throughout the process, competitive adsorption was effective with individual adsorption of the Cu and CN, where CN adsorption predominated. At pH 8–8.5, $[Cu(CN)_3]^{2-}$ was the predominant complex. At higher pH, all the Cu stayed in solution, complexed to CN (Bose *et al.*, 2002), so the complex was, therefore, adsorbed as an anion onto the surface, which resulted in smaller capacities compared to CN^- (Table 2).

FTIR spectroscopy

Fourier-transform infrared spectra of raw and Cu-complexed CN adsorbed minerals (Figure 9) revealed the effects of both acid activation and Cu-complexed CN adsorption on the mineral structure in the spectral interval of the $4000-400$ cm^{-1} interval, within which the main changes were observed in the $3700-3300$ cm^{-1} and $1200-400$ cm^{-1} intervals. The former is related to structural hydroxyl groups, while the latter reflects the mineral structure.

After acid treatment of zeolite, structural hydroxyl groups of the mineral (3740 cm^{-1} for silanol OH groups, ~3650 cm^{-1} for the bridging groups, and at 3550 cm^{-1} for extra-cage OH groups) in spectrum a (Figure 9) were decreased in intensity in spectrum c (Figure 9); the decrease represents a loss of zeolitic water. As well as the reduction in the absorption of water, acid treatment also caused some structural changes such that the $1200-950$ cm^{-1} band broadened and shifted (the bands are due to Si−O−Si and Si−O−Al vibrations); the frequency of the main asymmetric stretch at ~1040 cm^{-1} decreased, a distinctive shift at ~1000 cm^{-1} was observed, and many peaks for pseudo-lattice vibrations at $600-400$ cm^{-1} also disappeared. All these findings indicate that zeolite underwent dealumination.

Raw zeolite led to the greatest degree of Cu-complexed CN adsorption, and the most drastic changes were observed between spectra a and b in Figure 9. The intensity of the region representing structural hydroxyl groups decreased and the band broadened; the peak intensity at 1631 cm^{-1} decreased (OH bending) and the Si-O band 1049 cm^{-1} broadened; many peak intensities between 700 and 400 cm^{-1} decreased or vanished. All indicated the reduction of water in the structure and the entrance of Cu-complexed CN into the structure. Adsorption of this compound by acid-activated zeolite did not result in the same changes, as can be seen in spectra b and d (Figure 9). Peaks in the range $3700-3300$ cm^{-1} remained almost the same; a distinctive peak appeared at 2341 cm^{-1}, which was assigned to the C≡N triple bonds, and other changes were similar to those of raw zeolite.

In the high-wavenumber region, the bands assigned in the raw samples to ($Me-Me$)−OH ($3700-3500$ cm^{-1}) and to adsorbed water molecules ($3500-3200$ cm^{-1}) decreased with the intensity of the acid attack after acid activation of sepiolite (Figure 9g). The bands appeared at 3691, 3632, and 3567 cm^{-1} in sepiolite and are assigned to Al and Mg ions in the structure; a decrease in these bands was due to Mg dissolution during acid activation. A decrease in the bound-water band at 3520 cm^{-1} with a large broadening of the zeolitic water band at 3400 cm^{-1} were observed (Figure 9e,g). The changes seem to confirm the transformation of zeolitic and bound water to weakly-bound hydroxyl groups. A decrease in frequency of the 1660 cm^{-1} bending band was observed with acid treatment. The 1660 cm^{-1} band was also due to the bending vibration mode of water. Lattice vibrations in sepiolite were between the 1200 and 400 cm^{-1} region. Many bands characteristic of sepiolite in that region were observed in the raw sepiolite samples, which corresponded to Si−O and Me−O streching vibration bonds, and some disappeared or decreased in intensity due to dissolution of the octahedral sheet as acid treatment progressed. Peaks at 1210 and 980 cm^{-1} (Si−O combination bands) decreased, broadened, and almost disappeared after acid treatment indicating that structural degradation occurred in the tetrahedral sheet. The Si−O−Si in-plane vibrations at ~1020 cm^{-1} were also sensitive to acid treatment because they corresponded to the basal plane of the tetrahedral sheet. The $690-646$ cm^{-1} band pair represents a typical trioctahedral OH deformation which also reduced after acid treatment.
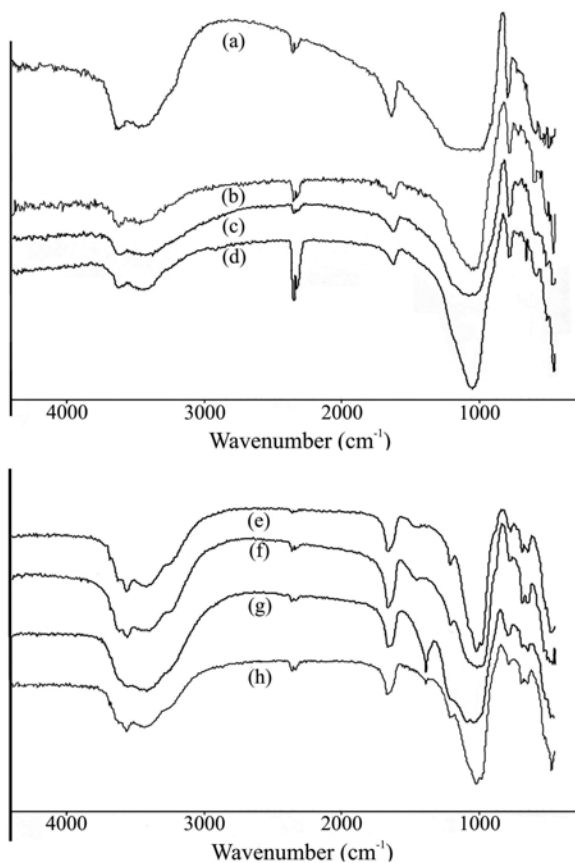
Figure 9. FTIR spectra of minerals: (a) raw zeolite; (b) raw zeolite after CuCN adsorption; (c) acid-activated zeolite; (d) acid-activated zeolite after CuCN adsorption; (e) raw sepiolite; (f) raw sepiolite after CuCN adsorption; (g) acid-activated sepiolite; (h) acid-activated sepiolite after CuCN adsorption.

The changes in raw sepiolite after Cu-complexed CN adsorption were significant (Figure 9e,f). The spectral changes observed in the $1200-400$ cm^{-1} region represent the lattice vibrations corresponding to Si−O, Si−O−Mg, and Mg−OH. The intensities of the $690-646$ pair increased, new peaks were formed at 490 and 526 cm^{-1}, and the peak at ~1020 cm^{-1} decreased. The bonding of CN in the structure, especially in the tetrahedral sheet, is indicated. In contrast, the adsorption of Cu-complexed CN onto acid-activated sepiolite could be followed from the changes in the $3700-3300$ cm^{-1} region. Unlike raw sepiolite, spectral changes, which were assigned to $(Me-Me)-OH$ and adsorbed water molecules, were observed in the $3700-3000$ range after adsorption of Cu-complexed CN onto acid-activated sepiolite. The changes in the $1200-400$ cm^{-1} region were less. The intensities of the $690-646$ cm^{-1} pair increased, a new peak was formed at 981 cm^{-1}, and the peak at ~1020 cm^{-1} increased.

CONCLUSIONS

Zeolite and sepiolite, both in raw and acid-activated forms, were effective at removal of cyanide from aqueous solutions, whether in the free form or the Cu-complexed form. In all conditions, up to 96% removal could be achieved. For removal of free CN, zeolite was more effective, for removal of Cu-complexed CN sepiolite performed better. Particle size was an important parameter in the cyanide-adsorption performance of sepiolite; smaller particle sizes (<0.106 mm) were better at removing CN$^-$. For zeolite, the influence of particle size was less. For both minerals, 1050 min was found to be the equilibrium time. The CEC values were large, as large as many other common adsorbents; the maximum CN$^-$ exchange capacities of zeolite and sepiolite were calculated as 571 and 695 meq/100 g, respectively. In the case of Cu-complexed CN, the capacities decreased to 455 and 435 meq/100 g for zeolite and sepiolite, respectively, due to competitive adsorption onto the mineral surface in the presence of Cu^{2+} ions.

Acid activation did not improve CN removal by these minerals; reductions of up to 25% in adsorption capacities were observed following the acid-activation process. Generally acid activation is acknowledged to increase adsorption capacities. In the present case, these decreases are thought to have been related to cation adsorption onto the minerals. Anion-adsorption capacity was not directly proportional to the surface area for CN removal. Instead, the surface structure is more effective.

The adsorption isotherm data indicated that most of the adsorption processes fitted the Langmuir isotherm, indicating monolayer coverage of the mineral surface with chemical bonding at uniform energy.

Removal of CN was not similar to simple cation adsorption; rather, anions were chemisorbed at the edge surfaces. Zeolite edge surfaces are similar to hydrous metal oxides of Si and Al; hydroxylated surfaces of these layers develop a pH-dependent charge on the surface, and these surface hydroxide ions exchange with the anions in an aqueous environment. In the sepiolite structure, Mg^{2+} ions located at the edges of the octahedral sheet and zeolitic water bonded to coordinated water molecules through hydrogen bonding. Complexation between these Mg^{2+} ions and CN anions and/or hydrogen-bonding anions and H$^+$ of bound water are the main mechanisms for sepiolite attraction of CN. Dissolution of Mg together with the octahedral sheet and a decrease in zeolitic water after acid activation are the main reasons for the decreases in the adsorption capacities. The effects of both acid activation and Cu-complexed CN adsorption on mineral structure were clearly observed as changes in the IR spectra.

The sepiolite and zeolite studied here are natural, plentiful, and cheap and may prove to be effective alternatives in the removal of free and Cu-complexed CN from aqueous solutions.

REFERENCES

APHA/AWWA/WPCF (1998) *Standard Methods for the Examination of Water and Wastewater.* 20th edition. Washington DC.

Baghel, A., Singh, B., Pandey, P., Dhaked, R.K., Gupta, A.K., Ganeshan, K., and Sekhar, K. (2006) Adsorptive removal of water poisons from contaminated water by adsorbents. *Journal of Hazardous Materials*, **B137**, 396−400.

Barakat, M.A. (2005) Adsorption behavior of copper and cyanide ions at TiO_2-solution interface. *Journal of Colloid and Interface Science*, **291**, 345−352.

Barrer, R.M. and Makki, M.B. (1964) Molecular sieve sorbents from clinoptilolite. *Canadian Jorunal of Chemistry*, **42**,1481−1487.

Bose, P., Aparna Bose, M., and Kumar, S. (2002) Critical evaluation of treatment strategies involving adsorption and chelation for wastewater containing copper, zinc and cyanide. *Advances in Environmental Research*, **7**, 179−185.

Brigatti, M.F., Franchini, G., Frigieri, P., Gardinali, C., Medici, L., and Poppi, L. (1999) Treatment of industrial wastewater using zeolite and sepiolite, natural microporous materials. *The Canadian Journal of Chemical Engineering*, **77**, 163−168.

Brigatti, M.F., Lugli, C., and Poppi, L. (2000) Kinetics of heavy metal removal and recovery in sepiolite. *Applied Clay Science*, **16**, 45−57.

Çetişli, H. and Gedikbey, T. (1990) Dissolution kinetics of sepiolite from Eskişehir (Turkey) in hydrochloric acid and nitric acids. *Clay Minerals*, **25**, 207−215.

Fujiwara, N., Liu, Y.L., Nakamura, T., Maida, O., Tabakashi, M., and Kabayashi, H. (2004) Removal of copper and nickel contaminants from Si surface by use of cyanide solutions. *Applied Clay Science*, **235**, 372−375.

Hernandez, L.G., Rueda, L.I., Diaz, A.R., and Anton, C.C. (1986) Preparation of amorphous silica by acid dissolution of sepiolite: Kinetic and textural study. *Journal of Colloid and Interface Science*, **109**, 150−160.

Kowalczyk, P., Sprynskyy, M., Terzyk, A.P., Lebedynets, M., Namie'snik, J., and Buszewski, B. (2006) Porous structure of natural and modified clinoptilolites. *Journal of Colloid and Interface Science*, **297**, 77−85.

Monser, L. and Adhoum, N. (2002) Modified activated carbon for the removal of copper, zinc, chromium and cyanide from wastewater. *Separation and Purification Technology*, **26**, 137−146.

Ou, B. and Zaidi, A. (1995) Cyanide − dispelling the myths − natural degradation. *Mining Environmental Management*, **June 1995**, 5−7.

Özdemir, O., Çınar, M., Sabah, E., Arslan, F., and Çelik, M.S. (2007) Adsorption of anionic surfactants onto sepiolite. *Journal of Hazardous Materials*, **147**, 625−632.

Reynolds, T.D. (1982) *Unit Operations and Processes in Environmental Engineering.* Wadsworth, California, USA, 576 pp.

Robbins, G. and Devuyst, E. (1995) Cyanide − dispelling the myths − Inco's SO_2/Air Process. *Mining Environmental Management*, **June 1995**, 8−9.

Rytwo, G., Nir, S., Margulies, L., Casal, B., Merino, J., Ruiz-Hitzky, E, and Serratosa, J.M. (1998) Adsorption of monovalent organic cations on sepiolite: experimental results and model calculations. *Clay and Clay Minerals*, **46**, 340−348.

Shariatmadari, H., Mermut, A.R., and Benke, M.B. (1999) Sorption of selected cationic and neutral organic molecules on palygorskite and sepiolite. *Clay and Clay Minerals*, **47**, 44−53.

Sujana, M.G., Pradhan, H.K., and Anand, S. (2009) Studies on sorption of some geomaterials for fluoride removal from aqueous solutions. *Journal of Hazardous Materials*, **161**, 120−125.

Tijburg, I.I.M. and Konuksever, A. (1998) Process for making aluminosilicate for record material. United States Patent Number 5,766,564; date of patent June 16, 1998. Assignee Akzo-PQ Silica VOF, Amersfoort, The Netherlands.

Van Olphen, H. (1959) Ion adsorption on clays: A review. *Clays and Clay Minerals*, **8**, 115 pp.

Vasylechko, V.O., Gryshchouk, G.V., Kuz'ma, Y.B., Zakordonskiy, V.P., Vasylechko, L.O., Lebedynets, L.O., and Kalytovs'ka, M.B., (2003) Adsorption of cadmium on acid-modified Transcarpathian clinoptilolite. *Microporous and Mesoporous Materials*, **60**, 183−196.

Waterland, R.A. (1995) Cyanide − dispelling the myths − Homestake's bio-treatment. *Mining Environmental Management*, **June 1995**, 12−13.

Yarar, B. (2001) Cyanides in the environment and their long-term fate. *Proceedings of 17th International Mining Congress and Exhibition of Turkey − IMCET2001*, pp. 85−93.

Young, C.A. and Jordan, T.S. (1995) Cyanide remediation: Current and past technologies. *Proceedings of the 10th Annual Conference on Hazardous Waste Research*, 104−129.